Bull. Astr. Soc. India (1998) **26**, 479-492

The central depth of the Ca II triplet lines as a discriminant of chromospheric activity in late type stars

Sushma V. Mallik
Indian Institute of Astrophysics, Bangalore 560 034, India

Abstract. A detailed analysis of the CCD spectra of the Ca II triplet lines λλ8498, 8542, 8662 obtained at a resolution of 0.4Å in 146 stars spanning all luminosities and a large range in spectral type and metallicity has shown that the Ca II triplet strength and depth are a good discriminant of luminosity, metallicity and chromospheric activity. In order to investigate the interdependence between chromospheric activity, age and lithium abundance, the Li I line at 6707.8Å has been observed in several chromospherically active and quiet stars from the above sample. The analysis reveals that there is no one-to-one correlation between Li abundance and chromospheric activity. A large range in Li abundances is observed both in active and quiet giants.

Key words : cool stars - chromospheric activity - lithium abundance

1. Introduction

The resonance lines Ca II H and K at λλ3933, 3968 have been traditionally used as diagnostics of luminosity and chromospheric activity in late F, G, K and M stars (Cassinelli & MacGregor 1986). The exposures of stars in these lines have to be deep enough to be able to record the emission components K_2 or the absorption components K_3 which originate in the chromosphere. Since the bulk of the continuum of these stars lies in the red, it is difficult to obtain good signal to noise level in the vicinity of these lines with a moderate size telescope. On the other hand, the infrared triplet lines of Ca II at λλ 8498, 8542, 8662 are ideally placed in the spectrum and are the most conspicuous features of the near infrared region of the spectra of the old stellar populations and the nuclei of galaxies predominantly characterised by G, K and M stars. There has been a large number of their studies in stars and galaxies to explain the dependence on stellar atmosphere parameters such as luminosity, temperature and metallicity (Jones et al. 1984, Carter et al. 1986, Diaz et al. 1989). This information has been exploited as a powerful tool for the study of stellar populations in galaxies.

2. Observations

In order to understand more completely the behaviour of the Ca II triplet line strengths, one has to study it over a large range of parameters. With this in mind, we sampled 146 stars from the Bright Star Catalogue (Hoffleit 1982) and the [Fe/H] Catalogue of Cayrel de Strobel et al. (1992) brighter than V = + 6.0 of all luminosity classes ranging in spectral types from F5 to M4 and in [Fe/H] from –3.0 to + 1.1 . The observations were obtained at the 102 cm telescope at VBO, Kavalur with the coudé echelle spectrograph and a 384 × 576 CCD, each pixel of 23μ square size. The spectrograph consisted of a $79 lmm^{-1}$ echelle grating, blazed at 6746 Å in the 34th order, a $150 lmm^{-1}$ cross dispersion grating blazed at 8000Å in the 1st order and a 250 mm camera. This configuration gave with the slit width chosen, a spectral resolution of ~ 0.4Å in the 26th order where the Ca II triplet lines lie.

Table 1 gives the stellar data and the EQWs determined of each line. The stellar parameters are from the [Fe/H] Catalogue. Here $\theta_{eff} = 5040 / T_{eff}$. CaT is the sum of the EQWs of all the three lines.

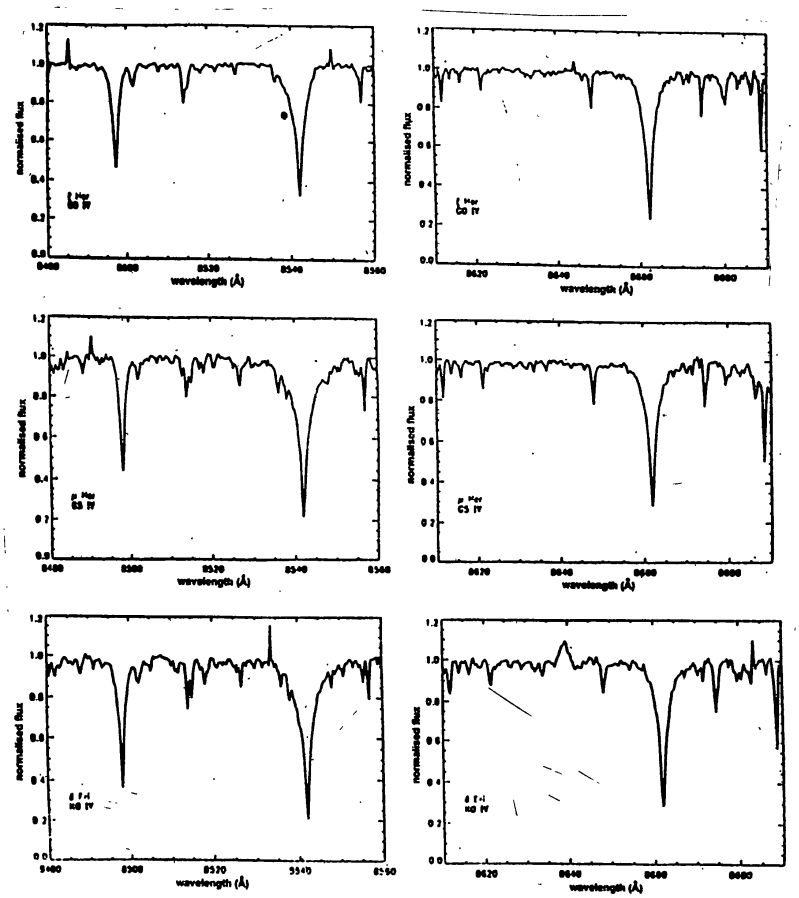

Figure 1. Spectra around the λλ8498, 8542, 8662 lines of Ca II for subgiants over a range of spectral types

Table 1. Stellar parameters and measured EQWs of the Ca II triplet

Star	Spectral type	θ_{eff}	R−I	log g	[Fe/H]	EQW(Å) λ8498	λ8542	λ8662	CaT (Å)
μ Cas	G5 V	0.95	0.42	4.5	−0.90	0.98	2.59	2.02	5.59
υ And	F8 V	0.84	0.29	3.91	−0.23	1.14	2.32	1.81	5.27
τ Cet	G8 V	0.96	0.47	4.50	−0.58	0.97	2.31	1.80	5.08
γ^1 And	K3 IIb	1.15	0.69	0.92	−0.23	2.05	3.61	3.42	9.08
6 Per	K0 III	1.08		2.25	−0.70	1.28	2.94	2.61	6.83
θ Per	F8 V	0.84	0.30	4.06	−0.15	0.82	3.04	2.12	5.98
η Per	K3 Ib	1.17	0.89	1.0	−0.15	2.52	4.59	3.96	11.07
ρ Per	M4 II	1.44	1.62	0.8	+0.05	1.65	3.47	2.87	7.99
ι Per	G0 V	0.84	0.29	4.0	+0.10	1.30	3.09	2.44	6.83
82 Eri	G8 V	0.94	0.40	4.17	−0.54	1.07	3.04	2.37	6.48
ϵ Eri	K2 V	1.01	0.46	4.80	−0.20	1.16	2.96	2.06	6.18
δ Eri	K0 IV	0.95	0.50	3.95	+0.05	1.39	3.37	2.32	7.08
HD23841	K1 II	1.12	0.49	1.30	−0.90	1.57	3.98	3.10	8.65
μ Per	G0 Ib	0.92	0.55	1.50	+0.15	1.99	4.88	3.56	10.43
o^2 Eri	K1 V	0.99	0.45	4.31	−0.34	1.32	3.11	2.38	6.81
α Tau	K5 III	1.31	0.94	1.5	+0.00	1.88	4.20	3.22	9.30
53 Eri	K2 IIIb		0.56	2.69		1.37	3.33	3.10	7.85
ι Aur	K3 II		0.82	1.66	+0.00	2.24	4.49	3.88	10.61
o^2 Ori	K2 III		0.63	2.69		1.30	3.25	2.89	7.44
π^6 Ori	K2 II		0.70	1.37*		1.87	4.77	3.60	10.24
ϵ Lep	K5 III		0.81	2.32		1.94	3.92	3.39	9.25
λ Aur	G2 IV-V	0.86	0.32	4.1	+0.30	1.59	3.34	2.41	7.34
β Lep	G5 II		0.44	2.2		1.50	3.03	2.69	7.22
ϕ^2 Ori	K0 III	1.10	0.55	2.40	−0.70	1.20	2.85	2.52	6.57
δ Lep	K0 III	1.10	0.56	2.50	−0.50	1.38	2.94	2.42	6.74
β Col	K2 III	1.10	0.58	2.69	+0.13	1.57	3.46	2.94	7.97
χ^1 Ori	G0 V	0.85	0.31	4.50	−0.05	0.90	1.66	1.58	4.14
α Ori	M1 Iab		1.28	0.00		2.32	5.01	4.23	11.56
δ Aur	K0 III		0.52	2.92		1.39	4.01	2.78	8.18
1 Gem	G7 III		0.45	3.08		1.43	3.99	2.94	8.36
HR 2140	K3 III	1.26	0.51	0.90	−0.60	1.55	4.10	3.26	8.91
η Gem	M3 III		1.31	1.50		1.85	3.89	3.36	9.10
γ Mon	K3 III		0.64	1.98*		1.67	3.70	2.83	8.20
HR 2269	K3 Ib	1.53	1.06	1.13	−0.07	1.59	3.40	3.36	8.35
μ Gem	M3 IIIab	1.40	1.38	1.08	+0.11	1.74	3.64	3.37	8.75
ψ^1 Aur	M0 Iab	1.65	1.07	1.0	+0.08	3.18	5.49	4.58	13.25
δ Col	G7 II		0.47	2.2		1.54	3.44	2.43	7.41
ϵ Gem	G8 Ib	1.10	0.61	0.8	−0.05	2.62	4.71	4.02	11.35
τ Pup	K1 III		0.60	2.31*		1.45	4.21	3.17	8.83
15 Lyn	G5 III		0.44	2.71*		1.28	3.28	2.46	7.02
θ CMa	K4 III	1.27	0.78	1.9	−0.03	1.49	2.94	2.62	7.05
o^1 CMa	K2 Iab	1.19	0.82	0.00	−0.11	2.24	4.99	4.83	12.06
41 Gem	K3 Ib	1.15	0.85	0.8	−0.21	2.05	4.66	4.08	10.79
σ CMa	K7 Iab		1.00	1.0		2.63	4.68	4.22	11.53
ζ Gem	G0 Ib	0.88	0.41	1.63	+0.33	1.76	4.66	4.35	10.77
δ CMa	F8 Ia	0.81	0.33	0.6	+0.19	2.78	6.35	5.01	14.14
HR 2764	K3 Ib	1.12	0.99	1.35	+0.15	2.19	4.94	3.89	11.02
π Pup	K3 Ib		0.91	1.13		2.16	4.35	3.94	10.45
ι Gem	G9 III	1.14	0.50		+0.16	1.52	3.91	3.05	8.48

Table 1 continued

Star	Spectral type	θ_{eff}	R−I	log g	[Fe/H]	EQW(Å) λ8498	λ8542	λ8662	CaT (Å)
σ Pup	K5 III		0.92	1.65*		1.74	4.35	3.03	9.12
HR 2883	F5 V	0.87	0.21	4.7	−1.60	0.95	2.28	1.78	5.01
υ Gem	M0 III		0.91	1.37*		1.99	4.21	3.23	
σ Gem	K1 III		0.58			1.31	3.23	2.09	6.63
κ Gem	G8 IIIa	1.14	0.45	3.05	−0.20	1.21	3.08	2.32	6.61
β Gem	K0 IIIb	1.05	0.50	2.6	−0.11	1.37	3.53	2.64	7.54
1 Pup	K3 Ib	1.17	0.97	1.3	+0.01	1.87	4.69	3.65	10.21
HR 3018	G0 V	0.88	0.23	4.1	−1.16	0.91	2.37	2.02	5.30
ξ Pup	G3 Ib	1.01	0.55	1.15	+0.24	2.59	5.71	3.97	12.27
HR 3080	K1 II		0.56	1.6		1.86	4.30	3.21	9.37
ρ Pup	F6 II	0.71	0.21	3.25	+0.54	1.56	2.97	2.44	6.97
o UMa	G5 III	0.97	0.45	2.3	−0.02	1.30	3.27	2.89	7.46
β Pyx	G7 Ib		0.48	1.45*		1.52	4.12	2.91	8.55
δ Cnc	K0 III		0.54	2.42*		1.21	2.93	2.65	6.79
ϵ Hya	G5 III	1.01	0.39	3.14		1.15	3.04	2.35	6.54
γ Pyx	K3 III		0.68	2.45		1.68	4.00	3.15	8.83
ζ Hya	G9 II	1.13	0.49	2.5	−0.12	1.61	4.04	2.88	8.52
HR 3578	F6 V	0.87	0.23	3.85	−1.05	0.85	2.25	1.78	4.88
λ Vel	K4 Ib	1.19	0.94	1.4	+0.23	2.57	5.45	4.54	12.56
HR 3664	G6 III	1.21		2.20	−0.85	1.25	2.94	2.21	6.40
HD81192	G8 III	1.10	0.54	2.75	−0.70	1.26	3.44	2.68	7.38
α Hya	K3 II	1.15	0.77	1.86	−0.19	1.93	4.81	3.31	10.05
ϵ Leo	G1 II	0.93	0.43	2.40	−0.13	1.32	3.87	2.98	8.17
1 Car	G8 Ia	0.99	0.68	1.5	+0.30	1.94	4.94	3.85	10.73
μ Leo	K0 III	1.17	1.58	2.20	+0.31	1.58	3.67	2.65	7.90
HR 4050	K3IIa	1.12	0.81	1.6	+0.54	2.03	3.63	2.83	8.49
γ Leo	K0 III	1.08	0.62	2.39	−0.35	1.41	3.59	2.78	7.78
μ UMa	M2 IIIab		0.96	1.35		1.63	4.29	3.93	9.85
37 LMi	G2 II		0.38	1.87		1.89	4.85	3.55	10.29
ν Hya	K2 III		0.64	2.69	−0.19	1.32	3.01	2.84	7.17
46 LMi	K0 III	1.07	0.54	2.5	−0.22	1.22	3.82	2.59	7.63
HR 4257	K0 II	1.00	0.50	3.22	−0.03	1.18	1.94	1.51	4.63
ψ UMa	K1 III	1.04	0.57	2.78	−0.07	1.60	4.01	3.13	8.74
HR 4337	G4 0-Ia	0.88	0.59	0.4	+0.32	4.29	8.52	5.95	18.76
72 Leo	M3 II		1.31	0.04		2.24	4.59	3.54	10.37
δ Crt	G8 III	1.04	0.60	2.48	−0.33	1.34	2.48	2.26	6.08
o^1 Cen	G3 0-Ia	1.01	0.66	0.19*		3.09	7.44	4.85	15.38
ξ Hya	G7 III	1.04	0.48	2.2	−0.10	1.65	3.71	2.48	7.84
HR 4511	G0 0-Ia	0.91	0.36	0.39*		3.06	8.93	3.98	15.97
χ UMa	K0 III	1.26	0.60	2.92	−0.65	0.96	3.74	2.58	7.28
HR 4523	G5 V	0.93	0.38	4.1	−0.70	1.03	2.85	2.04	5.92
β Vir	F9 V	0.83	0.28	4.1	+0.18	1.01	1.88	1.83	4.72
HR 4550	G9 VI	1.01	0.45	4.5	−1.40	0.88	2.43	1.89	5.20
o Vir	G8 IIIa	1.03	0.49	2.6	−0.39	1.42	3.62	2.48	7.52
16 Vir	K0 IIIb	1.17	0.61	2.3	−0.20	1.66	3.79	2.78	8.23
γ Cru	M3.5 III		1.41	1.5		1.73	4.62	3.10	9.45
β Crv	G5 III		0.44	2.2		1.40	3.99	2.73	8.04
δ Vir	M3 III	1.38	1.33	1.3	−0.09	1.59	3.37	3.05	8.01
ϵ Vir	G8 IIIb	1.01	0.45	2.7	+0.10	1.50	3.21	2.69	7.40

Table 1 continued

Star	Spectral type	θ_{eff}	R−I	log g	[Fe/H]	EQW(Å) λ8498	λ8542	λ8662	Ca/T (Å)
β Com	G0 V	0.85	0.30	4.4	+0.02	0.90	2.29	2.02	5.21
HR 5089	G9 Ib	1.29	0.59	1.86	−0.36	1.61	4.72	3.13	9.46
HR 5176	K2 III	1.25	0.57	1.1	−0.80	1.59	3.85	2.70	8.14
η Boo	G0 IV	0.81	0.29	3.8	+0.16	1.08	1.97	1.85	4.90
HR 5270	K3 II	1.12	0.58	0.75	−3.00	0.63	1.39	1.31	3.33
θ Cen	K0 IIIb	1.00	0.53	2.93	+0.04	1.24	2.94	2.62	6.80
HR 5317	F7 V	0.81		4.3	+1.01	1.17	3.40	2.17	6.74
α Boo	K1 IIIb	1.19	0.65	1.7	−0.60	1.37	3.65	2.62	6.80
φ Vir	G2 IV		0.37	3.9		1.06	2.36	2.01	5.43
ρ Boo	K3 III	1.19	0.65	1.2	−0.50	1.48	2.99	2.90	7.37
ϵ Boo	K0 II		0.52	2.5		1.82	3.81	3.16	8.79
58 Hya	K4 III*	1.26	0.76	1.0	−0.75	1.55	3.63	2.44	7.62
δ Boo	G8 III	1.05	0.51	2.70	−0.50	1.33	2.93	2.50	6.76
ι Dra	K2 III	1.11	0.60	2.6	+0.30	1.78	4.02	2.95	8.75
γ Lib	G8.5 III	1.08	0.55	2.25	−0.40	1.26	3.36	2.26	6.88
α Ser	K2 III	1.1	0.57	2.9	+0.37	1.31	3.36	3.04	7.71
θ Lib	G8.5 IIIb	1.04	0.52	2.91	−0.07	1.81	3.96	2.74	8.51
δ Oph	M0.5 III	1.37	1.03	1.4	+0.32	1.73	4.59	2.96	9.28
γ^1 Nor	F9 Ia	0.86		0.51*		2.72	7.08	4.95	14.75
β Her	G7 III	1.20	0.48	3.08	+0.18	1.36	4.33	2.84	8.53
HR 6152	G8 II	1.16	0.70	1.5	−0.62	1.60	3.65	2.70	7.95
ζ Her	G0 IV	0.89	0.32	3.8	−0.19	1.18	2.28	2.07	5.53
ϵ Sco	K2.5 III	1.12	0.60	2.5	−0.30	1.66	4.01	2.70	8.37
π Her	K3 II	0.93	0.73	4.1	+0.32	2.08	4.49	3.32	9.89
β Arae	K3 Ib	1.10	0.53	1.3	+0.50	2.36	5.26	4.00	11.62
β Dra	G2 Ib-IIa	0.94	0.48	1.35	+0.30	1.83	4.40	3.43	9.66
μ Her	G5 IV	0.93	0.38	4.1	+0.32	1.10	3.48	2.28	6.86
γ Dra	K5 III	1.18	0.85	1.55	−0.23	1.95	4.53	3.54	10.02
η Ser	K0 III-IV	1.02	0.50	3.23	−0.12	1.20	3.54	2.27	7.01
109 Her	K2.5 IIIab	1.11	0.60	2.6	−0.38	1.63	3.93	2.77	8.33
R Sct	G0 I-K0 I	1.14	0.77	0.0	−0.88	1.36	3.06	1.84	6.26
θ Lyr	K0 II	1.14	0.58	1.72	−0.20	2.20	5.09	3.35	10.64
31 Aql	G8 IV	0.89	0.31	4.00	+0.21	1.35	3.39	2.43	7.17
γ Aql	K3 II		0.78	2.4	+0.00	1.85	4.31	3.53	9.69
β Aql	G8 IV	0.96	0.49	3.79	−0.15	1.17	3.36	2.20	6.23
HR 7703	K3 V	1.03	0.49	4.5	−0.58	1.11	2.92	2.20	6.23
β Cap	F8 V	0.82	0.50	4.0	+0.62	1.78	4.27	2.84	8.89
η Cep	K0 IV	1.06	0.49	3.0	−0.50	1.34	3.02	2.11	6.47
ξ Cyg	K4 Ib	1.23	0.92	1.6	−0.01	2.52	5.53	3.92	11.97
ϵ Peg	K2 Ib	1.16	0.76	1.0	−0.03	2.37	5.71	3.90	11.98
μ Cep	M2 Iae	1.55	1.76	−0.72*		2.59	6.82	3.31	12.72
ζ Cep	K1.5 Ib	1.12	0.78	0.75	+0.22	2.60	5.17	4.51	12.28
σ Peg	F7 IV	0.81	1.11	3.67	−0.33	1.07	3.23	2.52	6.82
β Peg	M2 II-III		1.32	1.10	+0.20	1.82	4.18	2.87	8.87
56 Peg	G8 Ib	1.12	0.68	1.40	−0.20	1.50	3.43	2.85	7.78
λ And	G8 III-IV	1.25	0.57	2.30	−0.78	0.86	2.58	1.71	5.15
ρ Cas	F8 Ia	0.84	0.74	0.25	+0.05	2.71	6.72	5.24	14.67
3 Cet	K3 Ib	1.19	0.78	0.80	−0.20	2.11	4.66	3.63	10.40

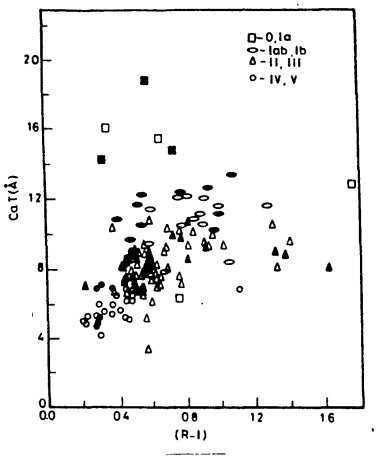

Figure 2. CaT versus (R – I). The filled symbols correspond to stars with [Fe/H] $\geq$ 0.0 whereas the unfilled ones to those with [Fe/H] < 0.0

3. Analysis of the data: dependence of the Ca II EQWs on stellar parameters

a) Temperature

Figure 1 shows the λλ8498, 8542, 8662 spectra for subgiants of roughly the same metallicity spread over a range of spectral types. Hardly any variation with spectral type is detected; this holds true for all luminosities and for both metal rich and metal poor stars. Figure 2 is the plot between CaT and (R–I). It is essentially a scatter diagram particularly in the case of giants and supergiants when seen separately. The conglomeration on the lower left part could be a selection effect; too many G and K giants and not many stars with large (R–I). It is important to cover a large enough parameter space; without a large span in (R–I), the plot tends to show only the gravity effect.

b) Surface gravity

Figure 3 shows spectra for F8 - G1 stars over the entire range of luminosities for stars of similar metallicity. A strong correlation exists between the Ca II strengths and luminosity. The lines are strong, wide and deep in supergiants and much weaker in dwarfs. One finds the same for all stars independent of metallicity and spectral type. Figure 4a shows the plot CaT - log g for the whole sample. The anticorrelation is non-linear, the slope sharply increasing with decreasing log g but flatter for subgiants and dwarfs. Jorgenson et al. (1992) have performed detailed non-LTE calculations of the Ca II triplet EQWs over a broad range of input parameters - log g : 0.0 – 4.0; T_{eff}: 4000 – 6600 K and Ca abundance : + 0.2 - –1.0. Their calculated relationship between EQW and log g represents a least squares, second order fit over the given range of log g. The observational data in the past have not led to a second order term in the fit because of fewer observations of luminous stars. Besides a large number of Ib supergiants, we have observed 8 superluminous supergiants. The plot clearly reveals an especially steep response for them. It is crucial to include these luminous

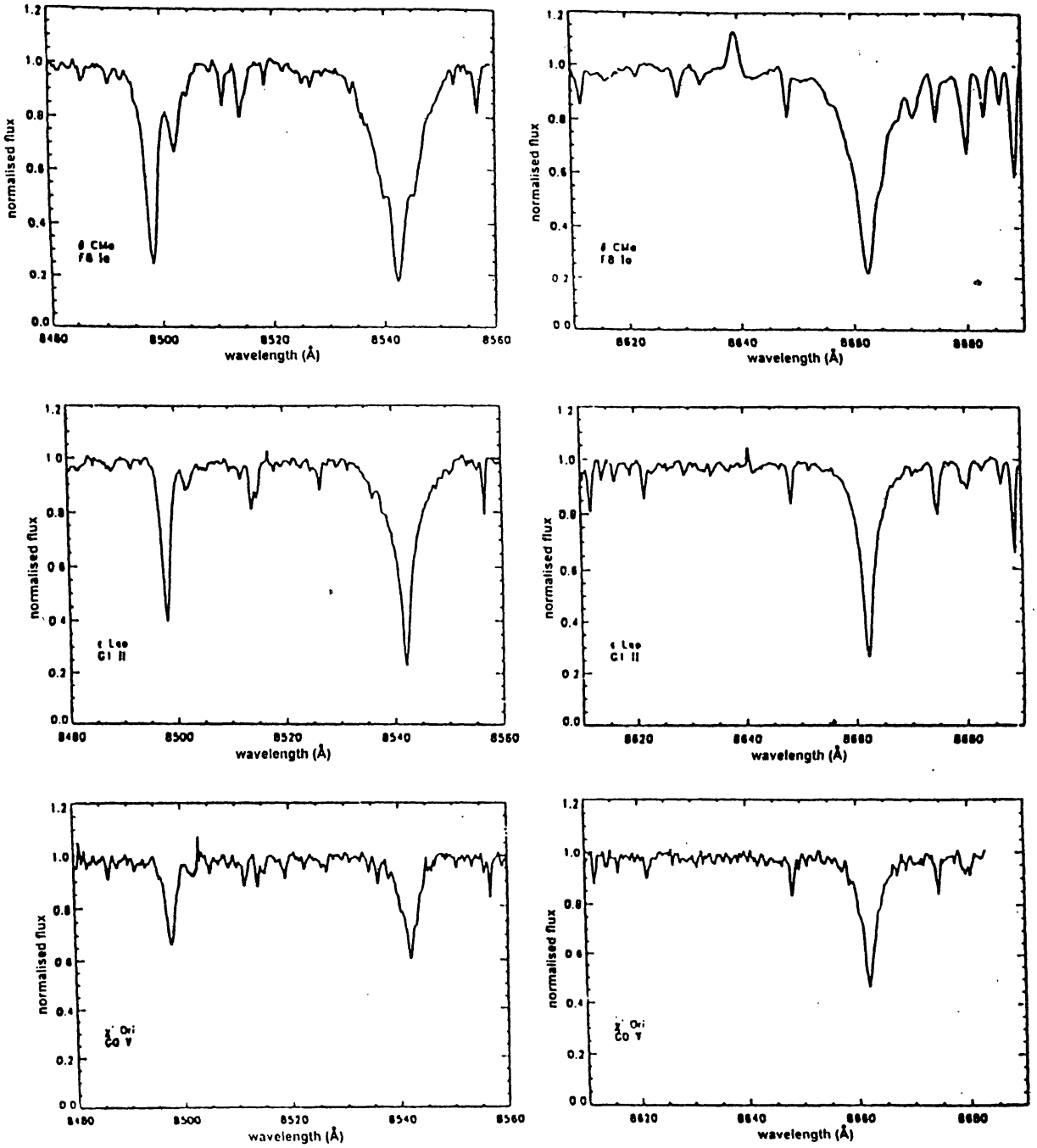

Figure 3. Spectra around the Ca II triplet lines for F8-G1 stars over a range of luminosities.

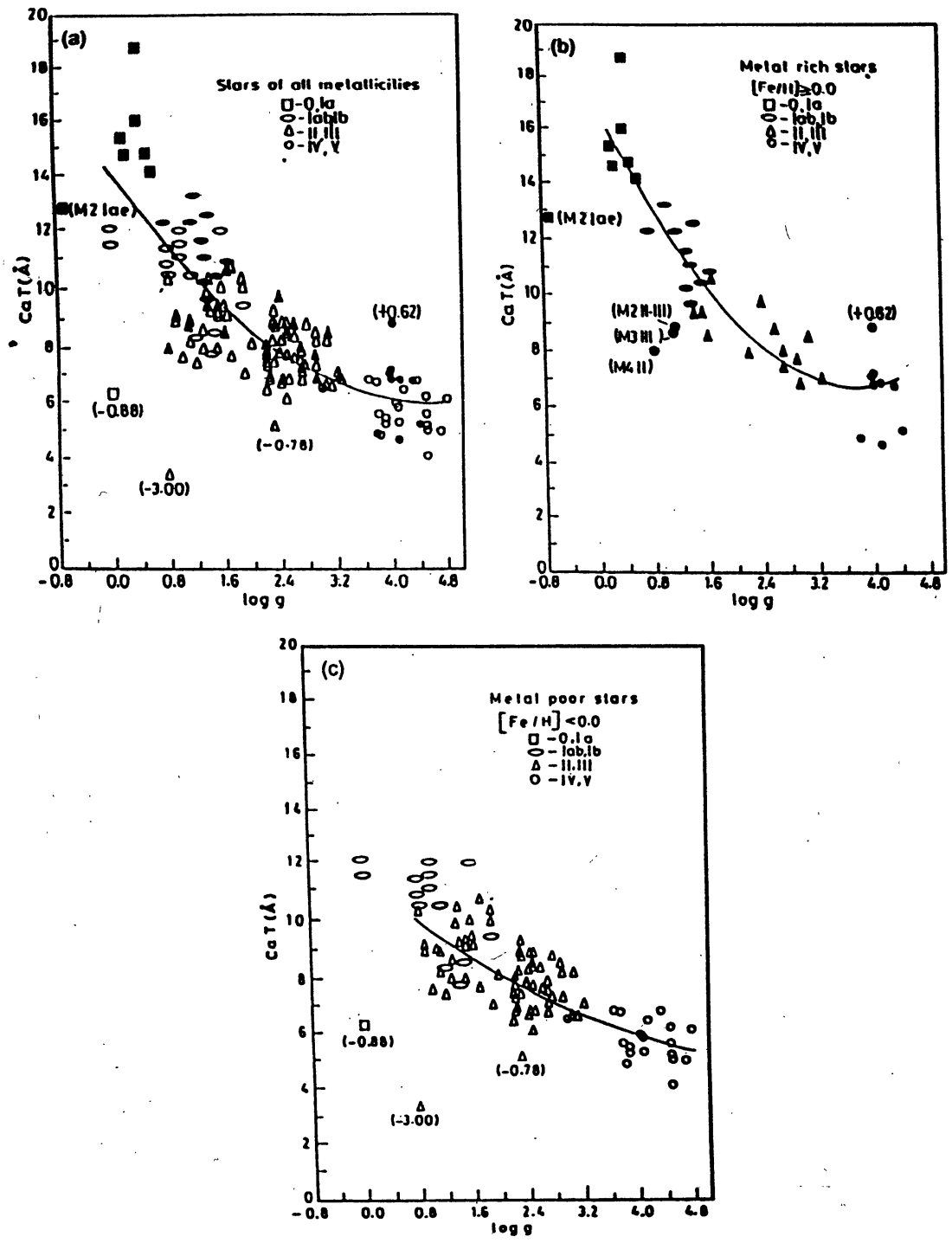

Figure 4. CaT versus log g for a : the whole star sample b : metal rich stars c: metal poor stars. The smooth curve drawn is a second order polynomial fit to the data points.

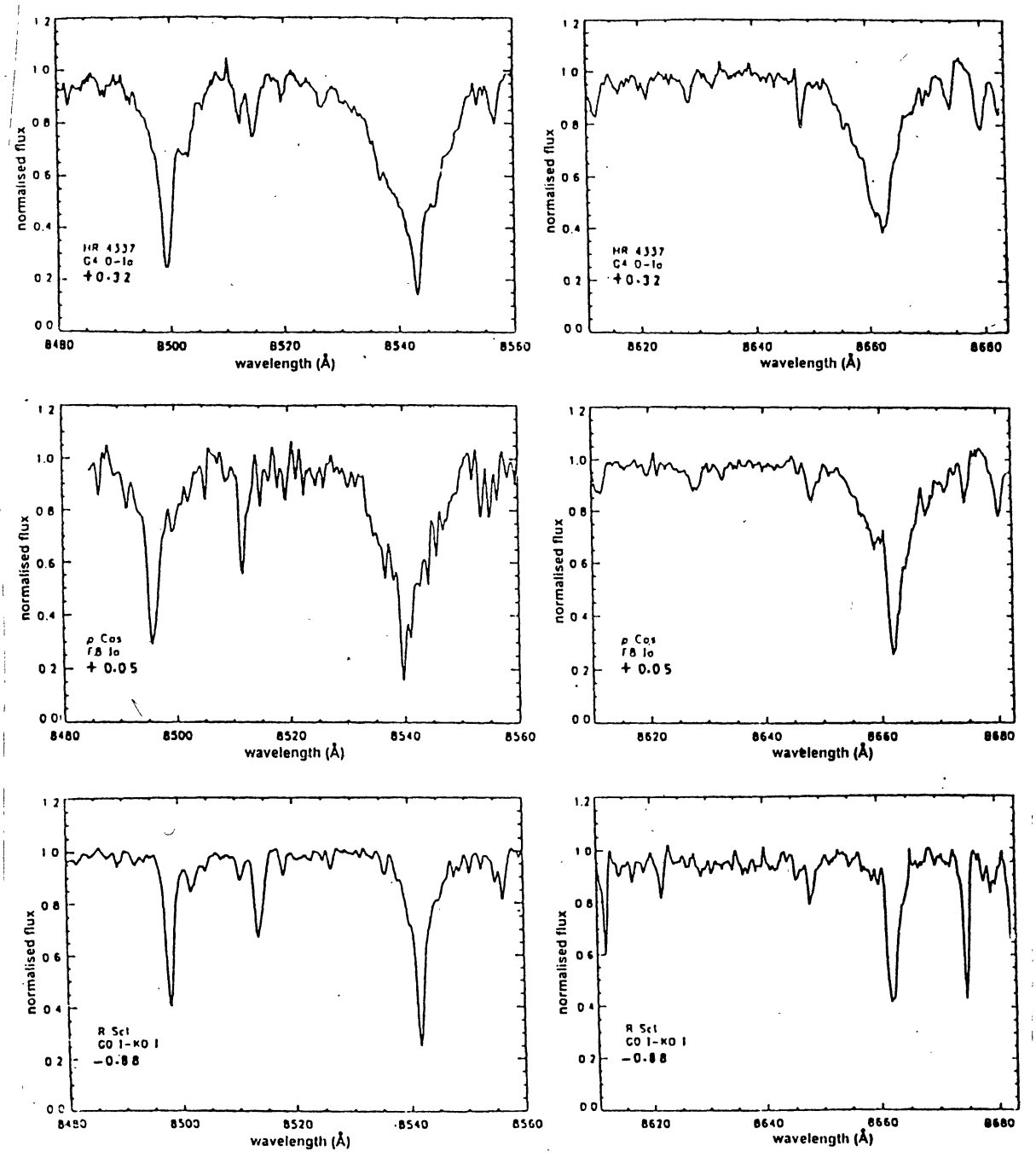

Figure 5. Sample sepctra of the Ca II lines for F8-G4 superluminous supergiants over a range of metallicity.

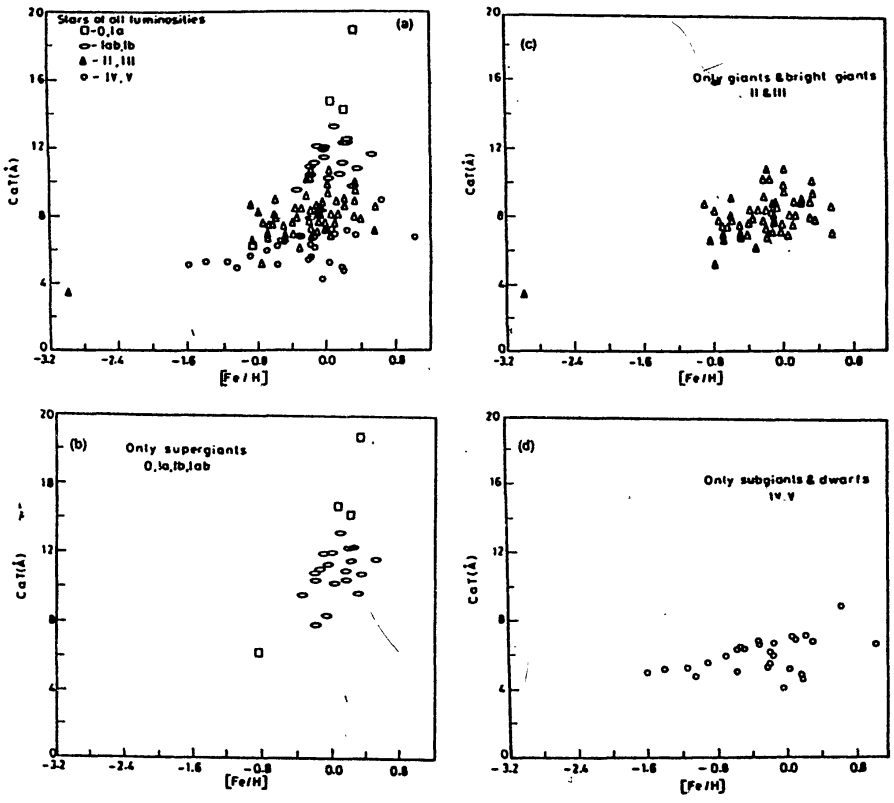

Figure 6. CaT versus [Fe/H] for a : the whole sample b : supergiants c : giants d : dwarfs

stars since they often contribute a large fraction to the integrated light from the external galaxies. A linear fit obtained from the less luminous stars would lead to an underestimate of the ratio of dwarfs to giants in a galaxy. Once again this shows the need to span as large a parameter space as possible. The solid curve drawn is a second order polynomial fit to the data points. Figures 4b and c are the plots separately drawn for metal rich and metal poor stars. A much tighter relation between CaT and log g exists for metal rich stars. Metal poor stars too have a non-linear response but not as steep. The stars that deviate are especially metal poor.

c) Metallicity

Figure 5 demonstrates how the strength of the Ca II triplet lines in F-G hypergiants relates to [Fe/H] over a range from + 0.32 to –0.88. They are much stronger in metal rich than in metal poor stars. Dwarfs because of the larger spread in age than supergiants are more likely to cover a larger range in [Fe/H]. In spite of this, the variation in the Ca II strengths is much more prominent in supergiants. Figure 6a gives the plot of CaT vs. [Fe /H] for the entire sample. Here the scatter is largely due to the luminosity effect. The response is non-linear. It is clear from Figures 6b, c and d that the CaT - [Fe / H] correlation is much stronger and steeper for supergiants than for dwarfs, even though the metallicity range covered is much less.

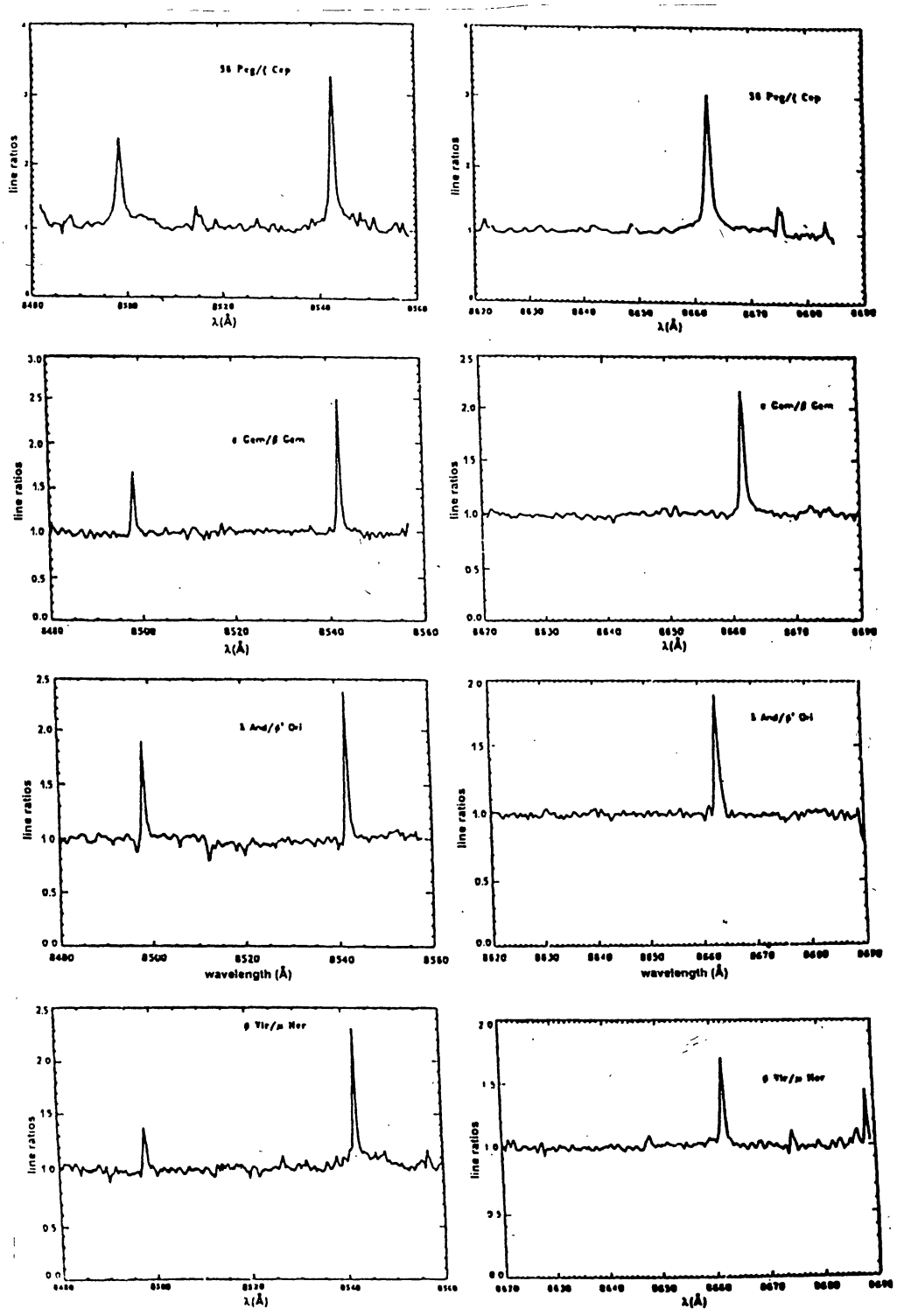

Figure 7. Line ratio spectra of λλ8498, 8542, 8662 for a few sample pairs.

d) Chromospheric activity and its relation to lithium abundance

Following the scheme of Linsky et al. (1979), we have arranged the observed spectra of stars into groups with similar spectral type, luminosity and metallicity and found that within a given group, there is often a star with higher central depth in the Ca II lines than the rest of the stars in that group. These are perhaps stars whose absorption profiles show filling in of the cores by unresolved chromospheric emission. 14 such stars were found. These are tabulated in Table 2 in form of pairs, the active followed by the inactive star. Column 3 has the activity index determined by Wilson (1976). For most of the stars $v \sin i$ is less than $20 km\ sec^{-1}$, so rotational broadening is not affecting the central depth. The central depths are higher and the EQWs are systematically lower for all the active stars. Figure 7 shows a sample of ratio spectra - the spectrum of the active star divided by the inactive one. These actually show the net emission in all the 3 lines, the amount that fills in the absorption of the Ca II triplet profiles in the star with higher chromospheric activity. Table 2 also lists the amount of this emission (FWHM multiplied by the peak emission value). It is interesting to note that it relates well to the luminosity of the star - it is higher for supergiants than for dwarfs, in analogy with the behaviour of the Ca II H and K line emission widths.

Cayrel de Strobel (1992) has observed the Ca II λλ8498, 8542 lines in a sample of nearby F, G and K dwarfs and slightly evolved subgiants to explore the stellar population of the nearest solar neighbourhood. This study revealed that in stars having the same temperature, the shallower the lines, more active is the chromosphere. Based on the assumption that such activity is tightly related to the age of the star, she used the central depth of the Ca II lines as a parameter for ranking the age of the observed disk stars and found a great difference in age between HD 100623 which turned out to be several billion years old and HD 17925 which is only a few million years old. Cayrel de Strobel & Cayrel (1989) had earlier detected a very strong Li line in HD 17925 which they interpreted as an indication that the star is very young. This observation is consistent with the star being chromospherically active. Since more than 98% of the stars in the solar neighbourhood belong to old disk population, it is a mystery where such a young star has come from. It is well known that even evolved stars like the RS CVn binaries and other giants are chromospherically active. Also, the Li abundance is not dictated by age alone. Therefore the above interpretation may not hold true in all situations.

We have recently undertaken a study of the Li I line at 6707.8Å in the 14 active stars and their counterparts. The CCD spectra in the Li I region have been obtained at a spectral resolution of ~0.35Å. A preliminary analysis shows that only 3 of the active stars are Li rich. An equal number of inactive stars is found to be more Li rich than their active counterparts. A large range in Li abundance is obtained both for the active and the inactive giants. This is most likely a consequence of the range in masses of their main sequence precursors. This interpretation decouples the Li problem from the star's activity and explains in a natural way the large range found in Li abundance in both active and quiet stars. We are extending our analysis to a much larger sample of stars to look further into the lithium problem.

Table 2. Summary of observations of star pairs

Star	Spectral	CRI			EQW(Å)			amount of emission in the divided spectra(Å)		
	type	λ8498	λ8542	λ8662	λ8498	λ8542	λ8662	λ8498	λ8542	λ8662
HR 2269	K3 Ib	0.32	0.25	0.30	1.59	3.40	3.36	2.06	2.54	3.58
3 Cet	K3 Ib	0.18	0.12	0.20	2.11	4.66	3.63			
HR 2269	K3 Ib	0.32	0.25	0.30	1 59	3.40	3.36	2.58	2.75	-
η Per	K3 Ib	0.17	0.12	0.08	2.52	4.59	3.96			
56 Peg	G8 Ib	0.45	0.35	0.24	1.50	3.43	2.85	3.54	3.74	3.74
ζ Cep	K1.5 Ib	0.16	0.11	0.10	2.60	5.17	4.51			
56 Peg	G8 Ib	0.45	0.35	0.24	1.50	3.43	2.85	2.77	3.38	4.08
ϵ Gem	G8 Ib	0.19	0.15	0.11	2.62	4.71	4.02			
β Dra	G2 Ib-IIa	0.37	0.27	0.31	1.83	4.40	3.43	2.15	1.33	2.50
ζ Gem	G0 Ib	0.28	0.15	0.15	1.76	4.66	4.35			
δ Vir	M3 III	0.33	0.20	0.17	1.59	3.37	3.05	1.35	1.75	1.31
η Gem	M3 III	0.28	0.14	0.18	1.85	3.89	3.36			
θ CMa	K4 III	0.30	0.17	0.16	1.49	2.94	2.62	1.06	1.45	1.25
α Tau	K5 III	0.25	0.12	0.13	1.88	4.20	3.22			
ν Hya	K2 III	0.33	0.23	0.18	1.32	3.01	2.84	1.20	1.40	-
β Col	K2 III	0.28	0.15	0.17	1.57	3.46	2.94			
σ Gem	K1 III	0.65	0.51	0.56	1.31	3.23	2.09	1.36	1.75	1.76
β Gem	K0 IIIb	0.37	0.17	0.23	1.37	3.53	2.64			
λ And	G8 III	0.73	0.57	0.58	0.86	2.58	1.71	1.52	1.80	1.58
ϕ^2 Ori	K0 III	0.37	0.20	0.23	1.20	2.85	2.52			
ϵ Hya	G5 III	0.5	0.33	0.36	1.15	3.04	2.35	1.21	1.37	1.83
o UMa	G5 III	0.38	0.21	0.12	1.30	3.27	2.21			
ϕ Vir	G2 IV	0.58	0.50	0.43	1.06	2.36	2.01	1.05	1.57	1.25
μ Her	G5 IV	0.45	0.22	0.29	1.10	3.48	2.28			
ϕ Vir	G2 IV	0.58	0.50	0.43	1.06	2.36	2.01	-	0.92	1.27
ζ Her	G0 IV	0.47	0.33	0.25	1.18	2.28	2.07			
ϵ Eri	K2 V	0.58	0.44	0.47	1.16	2.96	2.06	1.01	0.87	1.08
o^2 Eri	K1 V	0.50	0.32	0.33	1.32	3.11	2.38			
τ Cet	G8 V	0.54	0.40	0.43	0.97	2.31	1.80	1.44	0.96	0.80
82 Eri	G8 V	0.48	0.31	0.33	1.07	3.04	2.37			
χ^1 Ori	G0 V	0.66	0.60	0.46	0.90	1.66	1.58	1.17	1.09	1.47
β Com	G0 V	0.57	0.37	0.37	0.90	2.29	2.02			
χ^1 Ori	G0 V	0.66	0.60	0.46	0.90	1.66	1.58	1.14	1.56	1.57
β Vir	F9 V	0.50	0.35	0.33	1.10	1.88	1.83			
HR 5317	F7 V	0.58	0.37	0.32	1.17	3.40	2.17	2.34	2.62	-
β Cap	F8 V	0.36	0.21	0.21	1.78	4.27	2.84			

References

Carter, D., Visvanathan, N., Pickles, A.J. 1986, ApJ, 311, 637

Cassinelli, J. P., McGregor, K. B. 1986, Physics of the Sun, Vol III, ed. P. A. Sturrock, D. Reidel, p.47

Cayrel de Strobel, G. 1992, The ESO Messenger No. 70, ed. R.M. West, p.37

Cayrel de Strobel, G., Cayrel, R. 1989, A&A, 218, L 9

Cayrel de Strobel, G., Hauck, B., Francois, P. 1992, A&AS, 95, 273

Diaz, A.I., Terlevich,E., Terlevich, R. 1989, MNRAS, 239, 325.

Hoffleit,D. 1982, The Bright Star Catalogue, Fourth revised edition, Yale University Observatory, New Haven, Connecticut

Jones,J.E., Alloin, D.M., Jones, B.J.T. 1984, ApJ, 283, 457

Jorgenson, U.G., Carlsson,M., Johnson, H.R. 1992, A&A, 254, 258

Linsky,J.L., Hunten,D.M., Sowell, R., Glackin,D.L., Kelch, W.L. 1979, ApJS, 41, 481

Wilson, O.C. 1976, ApJ, 205, 823